Carbon dots derived from Arginine as metal free catalysts for rapid hydrogen production *via methanolysis of $NaBH_4$ with low activation energy*

By: Sahin Demirci, Betul Ari, Selin S. Suner, Nurettin Sahiner

https://doi.org/10.51167/acm00061

Arginine (Arg) based carbon dots (CDs) in the size range 0.5-10 nm as Arg-CD via microwave technique were prepared and were treated with HCl acid to protonate the amine groups on the structure, as Arg-CD$^+$. The surface charge of Arg-CD was increased to +21±1.2 mV for Arg-CD$^+$ from +2.8±0.5 mV. It was found that the Arg-CD$^+$ showed better catalytic activity than Arg-CD as catalyst in the methanolysis of $NaBH_4$ with higher hydrogen generation rate (HGR), 2534±128 mL H_2 x (g_{cat} x min)$^{-1}$ at 25°C. The Arg-CD$^+$ catalyzed methanolysis of $NaBH_4$ exhibited an HGR of 3233±151 mL H_2 x (g_{cat} x min)$^{-1}$ at 40°C. Furthermore, the activation energy values for and Arg-CD$^+$ in comparison to Arg-CD for the catalytic methanolysis of $NaBH_4$ was significantly decreased e.g., 10.9 kJ/mol versus 20.6 kJ/mol. Additionally, the a 50% activity was determined for Arg-CD$^+$ catalysts after five consecutive uses in methanolysis of $NaBH_4$ was almost recovered 100% recovered upon regeneration with a simple HCl acid treatment of the catalyst. The regeneration ability of Arg-CD$^+$ catalysts afforded 25 consecutive, effective, repetitive uses in methanolysis of $NaBH_4$ with more than 50% activity after every five cycles.

Sahin Demirci

Dr. Sahin Demirci received B.Sc. in Chemistry Department from Akdeniz University, Antalya, Türkiye, and M.Sc. Department at Canakkale Onsekiz Mart University (COMU), Canakkale, Türkiye. Dr. Demirci also completed his Ph.D. degree in Chemistry in 2021 at COMU under consultancy of Prof. Dr. Nurettin Sahiner. Dr. Demirci published over 80 peer-reviewed journal articles. His research interests include preparation of polymeric structures from synthetic and natural polymers at different dimensions, porosity, morphology and formulations and their composites with various inorganic and synthetic materials for applications in biomedicine, sensor, energy, environments, and catalysis.

Selin S. Suner

Dr. Selin S. Suner completed her Ph. D. degree under the supervision of Prof. Dr. Nurettin Sahiner in 2018 at Chemistry Department at Canakkale Onsekiz Mart University (COMU), Türkiye. She did Postdoctoral studies in Molecular Medicine at USF Morani College of Medicine in the USA. Currently, she is an Assistant Prof. Dr. in the Chemistry Department and Nanoscience and Technology Research and Application Center with Prof. Dr Sahiner at COMU. Her research interests include design of novel polymeric systems as antimicrobial, antioxidant, and anticancer materials, and delivery of therapeutics. She has 70 paper publication for the differemt polymeric systems for wide range of biomedical applications.

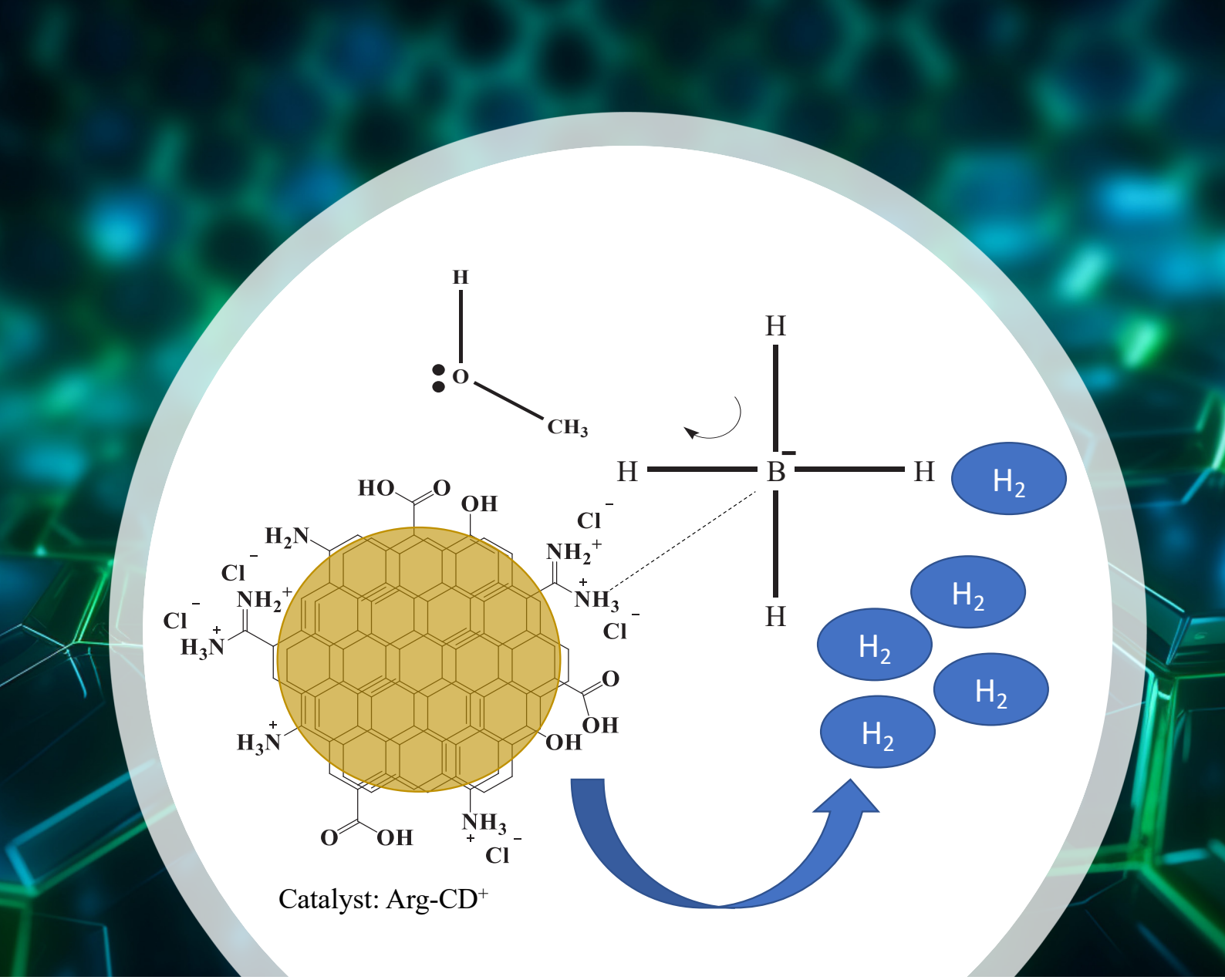

1. Introduction

Hydrogen (H_2) as an element is the lightest one in the periodic chart [1] and is the most commonly found element on Earth.[2] H_2 is regarded as a renewable energy source because it is clean, safe for the environment, carbon-free, and has an effective energy carrier.[3] H_2 is an alternative to replace fossil fuels because of the worldwide ecological effect of petroleum-based energy use and raising energy consumption and requirements.[2,4–6] At the same time, H_2 is more efficient than other fuels and has maximum energy content; for example, the energy content of H_2 is about 3 times the energy content of gasoline.[1] With the development of devices that use hydrogen as a fuel or energy source, there has been a need for carrier and storage systems.[7,8] In recent studies, various metal borohydrides ($NaBH_4$, $LiBH_4$, and NH_3BH_3)[9–16] have been widely used as H_2 storage materials to produce H_2. Moreover, various catalysts including metal nanoparticles and metal-free ones were also used to produce H_2 from $NaBH_4$ reactions as catalysts.[8,17].

Carbon based materials are also widely used as catalyst for $NaBH_4$ reaction in various solvents such as water or alcohol.[18–20] Active carbon, porous carbon, carbon nanotubes, graphitic carbon nitride ($g\text{-}C_3N_4$) et al., were intensively investigated as catalysts in different morphologies (porous, bulk etc.) and formulations (metal nanoparticle composites, doped, modified etc.) $NaBH_4$ reaction in various solvents such as water or alcohol to

Betul Ari
Betul Ari received her bachelor's degree in chemistry Dpt from Canakkale Onsekiz Mart University (COMU) and Master's degree from the same University under the supervision of Prof. Dr. Nurettin Sahiner. She is currently doing her PhD studies at the Chemistry Department at COMU. She has a total of 17 scientific publications, 14 in international peer-reviewed journal and 3 in national peer-reviewed journal.

Nurettin Sahiner
Dr. Sahiner received B.Sc. and M.Sc. degrees in Chemistry Department from Hacettepe University, Ankara, Türkiye, and Ph.D. degree in Chemical and Biomolecular Engineering at Tulane University, New Orleans, LA in 2005. He did his postdoctoral studies at the University of Delaware and Tulane University between 2005-2007 in Materials Sci. & Eng. and Biochemistry/Ophthalmology Dpts. Dr. Sahiner joined to Chemistry Department in Canakkale Onsekiz Mart University as an Assistant Professor in 2008 and become full professor in 2015. Dr. Sahiner holds several patents and published over 300 papers in peer reviewed scientific journals as well as several book chapters. He has presented his research work in many national and international conferences. His research interests include design of polymeric particles, hydrogels/cryogels and structures employing synthetic and natural polymers and molecules at different dimensions, porosity, morphology and formulations and their composites for applications in biomedicine, sensor, energy, environments and catalysis.

produce H_2.[20] The cost-effectiveness, environmentally benign nature, higher surface areas and so on render carbon based material unique advantages for the researchers to focused on catalytic applications of carbon based materials.[21,22] There are also report for the new type carbon based materials called 'carbon dots' with nano sizes, e.g., in 0.5-50 nm range with some extra additional assets such as conductivity, and fluorescent properties.[23,24] The optic properties of CDs make them light-sensitive structures with the possibility of photocatalyst materials in various application including energy, sensor, biomedical, and environmental uses.[23,25–28]

In this study, the synthesis of arginine-based N-doped carbon dots (Arg-CDs) via microwave technique were reported and their use for H_2 production from $NaBH_4$ were examined. The Arg-CDs were protonated due to the presence of amine groups on the structure upon HCl treatment and the catalytic performance on H_2 production was compared with untreated Arg-CD as catalysts. The effect of protonation, temperature, $NaBH_4$ concentration, and catalyst amount on catalytic activity of Arg-CDs based catalyst were investigated. The H_2 generation rate (HGR), and important activation parameters (Ea, ΔH, and ΔS) for Arg-CD based catalysts catalyzed $NaBH_4$ methanolysis reactions were determined. Moreover, the repetitive use and regeneration ability of Arg-CD$^+$ catalyst were tested.

2. Experimental

2.1 Materials

Citric acid monohydrate (CA, >99%, Carlo Erba, France) and L-Arginine (>98%, Sigma Aldrich, USA) were used for synthesis of Arg-CDs. Hydrochloric acid (HCl, 37.5%, Sigma Aldrich, USA) was used to protonate Arg-CDs. Acetone (96%, Birkim, Türkiye) were used for the precipitation of the prepared Arg-CDs. Sodium borohydride ($NaBH_4$, ≥98%, Merck, Germany) was used as hydrogen (H_2) carrier, and methanol (99%, Carlo Erba, France) was used as a solvent for H_2 production reactions.

2.2 Synthesis, characterization and catalytic use of Arg-CDs

The synthesis of Arg-CD was done in accordance with the research that was already been published [29,30]. The Fourier Transform Infrared Radiation (FT-IR, Thermo Nicolet iS10), Thermal gravimetric analysis (SII TG/DTA 6300, EXSTAR), and fluorescence spectrophotometer (Thermo Scientific, Lumina, USA) were used to characterize prepared Arg-CDs.

Catalytic performances of Arg-CDs were tested in H_2 generation studies from methanolysis of $NaBH_4$. The effect of protonation, the amount of catalyst (10-50 mg), the concentration of $NaBH_4$ (62.5-250 mM), the reaction temperature (-10 - +40 °C) on catalytic activity of catalysts in reaction were also tested. The important activation parameters, Ea, ΔH, and ΔS were also calculated from the well-known Arrhenius and Eyring equations (Eq. (1), and Eq (2)), respectively.

$$\ln k = -(E_a/RT) \times (1/T) \ln A \quad (1)$$

$$\ln (k/T) = -(\Delta H/R)(1/T) + \ln (k_B/h) + \Delta S/R \quad (2)$$

where k is the reaction's rate constant, Ea is its activation energy, T is its absolute temperature, k_B is its Boltzmann constant at 1.381×10^{-23} JK^{-1}, and h is its Planck constant at 6.626 10-34 Js; additionally, ΔH is its activation enthalpy, ΔS is its activation entropy, and R is its gas constant at 8.314 $JK^{-1}mol^{-1}$.

Moreover, the reusability, and regeneration ability of Arg-CD based catalyst were also tested via following literature[31].

3. Results and Discussion

3.1 Preparation and optical properties of Arg-CD and Arg-CD+ catalysts

The Arg-CDs were synthesized by our group via microwave methods in earlier studies,[29,30] and the corresponding schematic presentation of CD formation is given in **Figure 1**. The prepared Arg-CD possesses amine groups in the structure due to amine-rich starting material amino acid, arginine (Arg). Arg contains 3 moles of primary, and 1 mole of secondary amine groups per 1 mol of Arg molecule. Previously, the prepared Arg-CDs and its' metal nanoparticle composite were used for enhanced antibacterial activity,[30] and the augmentation of modified Arg-CDs upon light-activation in their antibacterial properties.[29]

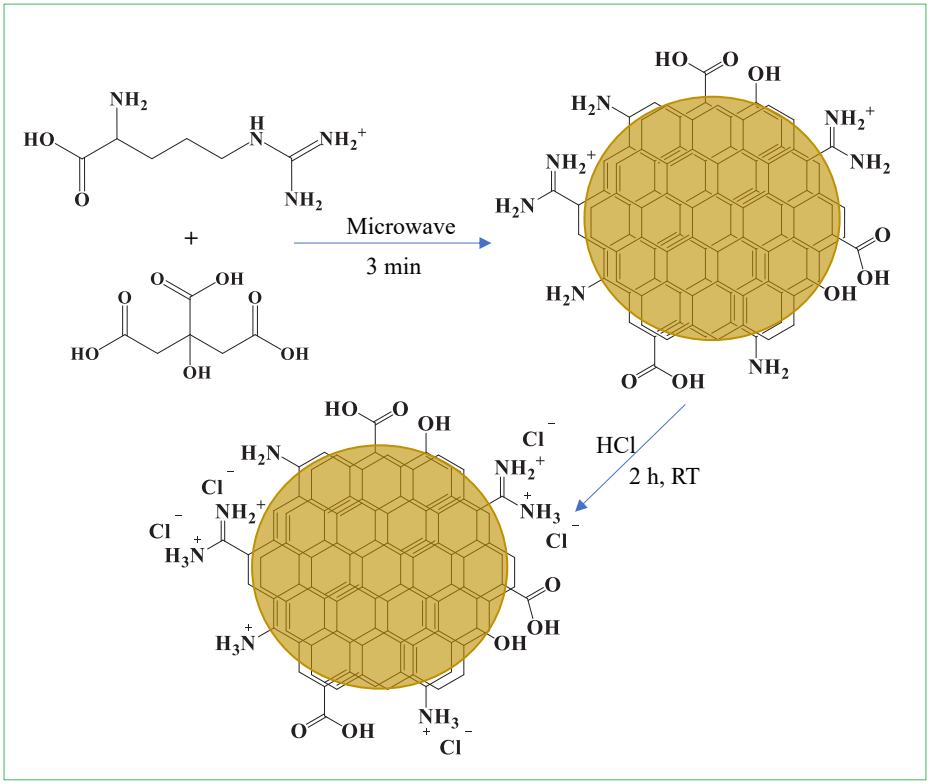

Figure 1. The schematic presentation of synthesis and protonation of Arg-CDs.

A complete characterization of Arg-CDs was also reported in earlier research.[29,30] Arg-CDs have an isoelectronic point of pH 4.1 with a zeta potential value of +2.8±0.5 mV.[29,30] An acid treatment was commonly used to protonate the amine groups on the Arg-CD particle. In comparison to neat Arg-CD (untreated with HCl), which had a zeta potential value of +2.8±0.5 mV, the protonation of Arg-CD generated a higher zeta potential value, +21±1.2 mV.

The structural, thermal, and optical properties of prepared Arg-CD and Arg-CD$^+$ were analyzed via FT-IR, TGA, and fluorescence spectra, spectroscopy and given **Figure 2**. In **Figure 2 (a)**, the FT-IR spectra of Arg, Arg-CD, and Arg-CD$^+$ were compared. The characteristic peaks for Arg amino acid such as aliphatic CH_2 at 2932 and 2848 cm^{-1}, C=O stretching at 1678 cm^{-1}, NH_2 asymmetric bending at 1620 cm^{-1}, COO^- symmetric stretching at 1425 cm^{-1}, and NH_2 asymmetric rocking at 1192 and 1136 cm^{-1}, respectively are clearly seen.[32,33] From the FT-IR spectra of Arg-CD and Arg-CD$^+$, the peaks for C=O

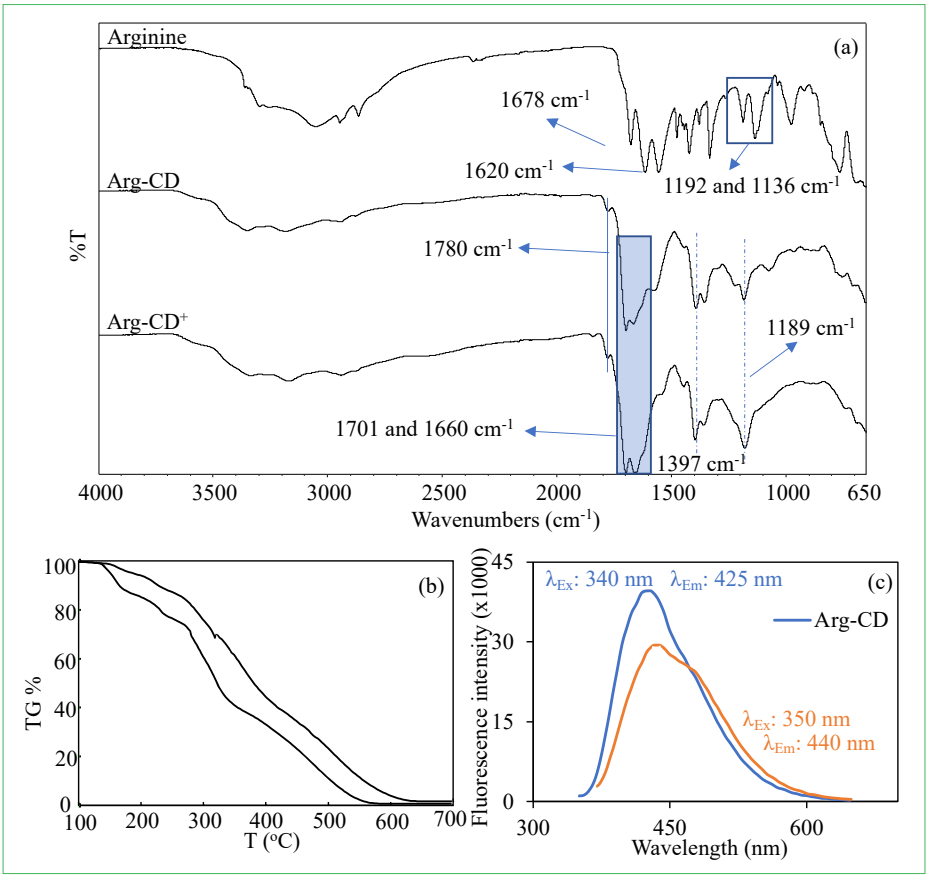

Figure 2. The comparison of (a) FT-IR spectra, (b) TGA thermograms, and (c) Fluorescence spectrums of Arg-CD and Arg-CD⁺.

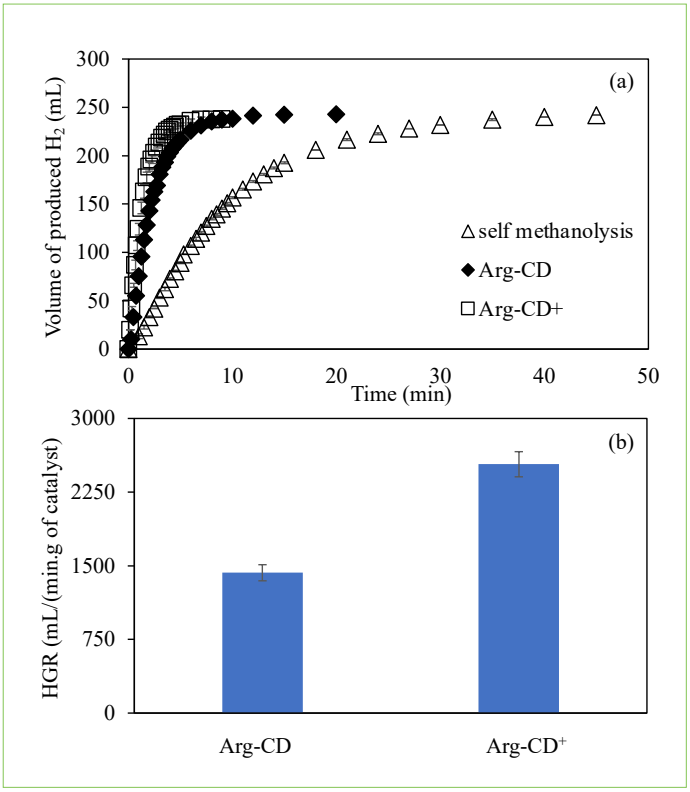

Figure 3. The methanolysis of $NaBH_4$ to produce H_2 using (a) self-methanolysis and Arg-CDs, and (b) a comparison of the HGR values for Arg-CD and Arg-CD⁺ catalyzed processes [Reaction condition: 20 mL methanol, 0.0965 g $NaBH_4$, 50 mg catalyst, 1000 rpm, 25°C].

stretching at 1780 and 1701 cm^{-1}, NH_2 bending at 1660 cm^{-1}, C-N stretching vibration at 1397 cm^{-1}, and NH_2 rocking at 1189 cm^{-1} were observed also exist.[29] The NH_2 bending peak intensity at 1660 cm^{-1} increased after protonation of Arg-CDs.

In **Figure 2 (b)**, the TGA thermogram compared the thermal stabilities of prepared Arg-CD and Arg-CD⁺ particles. It was clearly seen that the Arg-CD was thermally stable up to 200 °C and degraded in one step between 200-630 °C with >95% weight loss. On the other hand, Arg-CD⁺ started to degrade between 140-160 °C with almost 10% weight loss, then the second degradation step was observed between 180-270 °C with 28% cumulative weight loss, and the last degradation step between 280-560 °C with more than 99% cumulative weight loss was seen. The fluorescence spectrum of Arg-CD and Arg-CD⁺ was also given in **Figure 2 (c)**. The excitation wavelength of Arg-CD at 340 nm, shifted to 350 nm after preparation Arg-CD⁺. Moreover, the emission wavelength for Arg-CD and Arg-CD⁺ at related emission wavelengths were determined as 425, and 440 nm, respectively. The fluorescence intensity, and calculated QY% values for Arg-CD and Arg-CD⁺ were also compared in **Table 1**.

Table 1. The comparison of fluorescence intensity and QY% values for Arg-CD, and Arg-CD⁺.

Materials	Fluorescence intensity (a.u)	Quantum Yield (%)
Arg-CD	39620	2±33
Arg-CD⁺	29300	21±1

The fluorescence intensity of Arg-CD is 39620 reduced upon protonation and measured as 29300 at 500 V PMT voltage for Arg-CD⁺. Similarly, the calculated QY% values, based on 0.5 M quinine sulfate as standard, for Arg-CD is 32±3 is reduced to 21±1% for Arg-CD⁺. This is plausible as the present of hydronium ions in the structure increase the non-irradiative loss of energy for excited atoms.

3.2 H_2 production in the presence of Arg-CD and Arg-CD+ as catalysts

The suggested mechanism for metal-free amine based catalysis of reaction is Michaelis-Menten type mechanism and was reported in the literature with details.[34,35] Arg-CDs with amine groups in their structure were utilized as catalysts to generate H_2 from the reaction because these materials having amine groups have strong catalytic activity in the process. In addition, the benign nature (e.g., biocompatibility) of Arg-CDs render added motivation to use CDs particles as catalyst for clean energy generation tools. In **Figure 3 (a),** the self-methanolysis of $NaBH_4$ (without catalysts) is given and as seen this reaction was completed in 45 min with 250±2 mL H_2 production. On the other hand, the self-methanolysis of $NaBH_4$ 3-times accelerated in the presence of Arg-CD as catalyst, and the reaction completed in 15 min. In addition, 250±2 mL H_2 production was

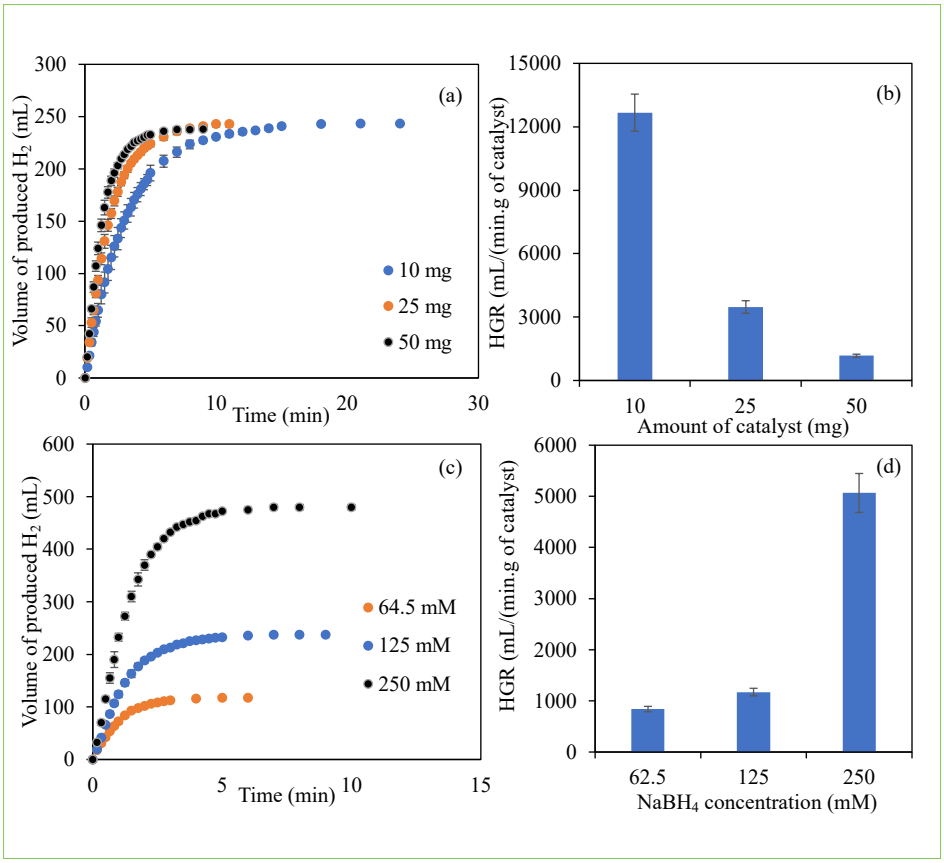

Figure 4. The effect of amount of catalyst on (a) hydrogen production with time, (b) the change in HGR values with different amounts of catalyst, (c) the effect of concentration of $NaBH_4$ on hydrogen production, and (d) the change in HGR values with amounts of $NaBH_4$ [Reaction condition, Arg-CD⁺ as catalyst, 20 mL methanol, $NaBH_4$, 25 °C, 1000 rpm].

observed in 7 min for the Arg-CD⁺ used as catalyst. So, the Arg-CD⁺ catalyzed reaction is almost 2-times faster than the Arg-CD catalyzed reaction.

Moreover, the HGR values for Arg-CD and Arg-CD⁺ catalyzed reaction is presented in **Figure 3 (b)**. It was observed that the calculated HGR value for Arg-CD⁺ catalyzed reaction as 2534±128 min^{-1} is higher than Arg-CD catalyzed reaction, 1429±82 min^{-1}. The increase on catalytic activity of Arg-CD⁺ catalyzed reaction can be explained by easy release of H_2 from the BH_4^- anion after interaction with the protonated amine groups on Arg-CD⁺.[34,35]

Moreover, Arg-CD⁺ catalyzed reaction in the presence of different catalyst amounts, $NaBH_4$ concentrations were also investigated, and the resulting graphs are provided in **Figure 4**. In **Figure 4 (a)**, the effect of amount of Arg-CD⁺ catalyst in reaction showed that the decrease in the amount of Arg-CD⁺ catalyst resulted in an increase in time to complete the reaction. For the reactions catalyzed by 10, 25, and 50 mg of Arg-CD⁺, the corresponding reactions were completed in 21, 11, and 7 min, respectively each producing 250±2 mL of H_2. On the other hand, the HGR values were compared in **Figure 4 (b).** As it can be seen the decrease in the amount of catalyst increased the HGR values. The HGR values were calculated as about 12700, 3500, and 1200 mL H_2 x $(g_{cat}$ x min$)^{-1}$ for 10, 25, and 50 mg Arg-CD⁺ catalyzed reactions, respectively. There was no direct proportion between the decrease in the amount of catalyst and the increase in the reaction completion time. However, the HGR values , and the reaction starts rapidly as the reaction proceeds the probability of collision of $NaBH_4$ with the catalyst decreases as the amount of $NaBH_4$ decreases in the medium.

Moreover, the concentration effect of $NaBH_4$ was also studied for H_2 production reaction in the presence of 50 mg of Arg-CD⁺ catalyst at 25 °C, and corresponding graph is given in **Figure 4 (c)**. It is obvious that $NaBH_4$ concentration did not affect the completion of reaction as each resulted in 100% conversions (stoichiometrically). The H_2 production from Arg-CD⁺ catalyzed 62.5, 125, and 500 mM $NaBH_4$ solution in methanol were completed in 6, 7, and 8 min with 123±2, 250±2, and 490±5 mL H_2 productions, respectively. Their HGR values are presented in **Figure 4 (d)**. It is clear that the HGR values were increased with the increase in the concentration of $NaBH_4$. The HGR values were calculated as 1512±101, 2534±128, and 5066±187 mL H_2 x $(g_{cat}$ x min$)^{-1}$ for 62.5, 125, and 500 mM $NaBH_4$, respectively. This is reasonable as the increasing in collision probability of catalyst and $NaBH_4$ is increased with the increase in the concentration of $NaBH_4$.

3.3 Activation parameters of Arg-CD and Arg-CD⁺ catalyzed reaction

The activation energy (E_a), enthalpy (ΔH), and entropy (ΔS) as important activation parameters were calculated for the reaction catalyzed by Arg-CD based materials by carrying the reactions at different temperatures. For this purpose, the reaction catalyzed by Arg-CD and Arg-CD⁺ were done at different temperatures ranging-10 - +40 °C, and the related graphs are given in **Figure 5 (a)**, and **(b)** respectively. In **Figure 5 (a)**, the reaction catalyzed by Arg-CD produced 250±2 mL H_2 in 40, 30, 21, 15, and 7 min at -10, 0, 10, 25, and 40 °C, respectively. The calculated HGR values for Arg-CD catalyzed reaction decreased from 1806±106 mL H_2 x $(g_{cat}$ x min$)^{-1}$ to 364±29 mL H_2 x $(g_{cat}$ x min$)^{-1}$ with the decrease of reaction temperature from 40 to -10 °C. Similarly, the reaction completion time for Arg-CD⁺ catalyzed reaction decreased with the decrease in temperature from 40 to -10 °C, and the related graph is illustrated in **Figure 5 (b)**. The Arg-CD⁺ catalyzed reaction conducted at -10, 0, 10, 25, and 40 °C completed with 250±2 mL H_2 production in 21, 18, 14, 7 and 5 min, respectively. Their HGR values at -10, 0, 10, 25, and 40 °C were also calculated and determined as 1245±53, 1632±33, 1798±87, 2534±128, and 3233±151 mL H_2 x $(g_{cat}$ x min$)^{-1}$, respectively. As can be seen from **Figure 5 (a)**, and **(b)** the reaction rates and HGR values were found to increase with increase in reaction temperature as expected.

Moreover, the Arrhenius and Eyring graphs for Arg-CD and Arg-CD⁺ as catalyzed reactions to calculate activation parameters are plotted and presented in **Figure 5 (c)**, and **(d)**, respectively. The calculated E_a, ΔH, and ΔS values for Arg-CD catalyzed reaction are 20.6 kJ/mol, 17.8 kJ/mol, and -175 J/(K x mol), respectively whereas the same parameters were calculated as 10.9 kJ/mol, 8.4 kJ/mol, and -148 J/(K x mol) for Arg-CD⁺ as catalyst. The calculated E_a values for Arg-CD and Arg-CD⁺ as catalyzed reaction as 20.6 and 10.9 kJ/mol were compared with some of the similar studies in literature and compared in **Table 2**.

Table 2. The comparison of Ea values of Arg-CD and Arg-CD⁺ catalyzed the reaction with the literature.

Catalysts	Ea (kJ/mol)	Ref
Arg-CD	20.6	This study
Arg-CD+	10.9	
S-AC-S-N	10.59	[36]
AC	11.76	[37]
P doped g-C3N4	30.29	[38]
P doped PPCD	30.96	[39]
Co-Mo-P / CNTs-Ni	47.27	[40]
Co-P/CNTs-Ni	49.94	[41]
mpg-CN/ BP-AgPd-aat	55.1	[42]

In literature, the reported E_a values for reaction catalyzed by various catalysts are 10.6 kJ/mol for S and N-doped metal-free carbon materials,[36] 11.8 kJ/mol for sawdust-based biomass-derived activated carbon catalyst,[37] 30.3 kJ/mol for P-doped g-C_3N_4 catalyst,[38] 31.0 kJ/mol for P-doped carbon nanodots catalyst,[39] 47.3 kJ/mol for dandelion-like CNTs-Ni foam composite carrier supported Co-Mo-P ternary alloy catalyst,[40] 49.9 kJ/mol for dandelion-like CNTs-Ni foam composite carrier supported Co-P as catalyst,[41] and 55.1 kJ/mol for mesoporous graphitic carbon nitride/black phosphorus-Ag/Pd as catalyst.[42] It is apparent that the reaction catalyzed by Arg-CD⁺ catalyst with 10.9 kJ/mol of activation energy is amongst the lowest ones reported in the literature. Therefore, the catalysts based on Arg-CDs have the potential to compete with the other carbon-based materials reported in the literature and possesses promising potential as catalyst not only because of catalytic performance but also its green nature.

3.4 Reusability and regeneration ability of Arg-CD⁺ catalyst in reaction

Among the various parameters for the determination of cost-effectiveness of catalyst that determines their industrial application potential is their reusability and regeneration capability. Therefore, the repetitive usage and regeneration ability of Arg-CD⁺ catalyst in reaction were tested and corresponding graphs are illustrated in **Figure 6 (a)** and **(b),** respectively. It was observed that the reaction catalyzed by Arg-CD⁺ can complete 100% conversion for each use up to consecutive uses. On the other hand, the activity% of Arg-CD⁺ catalyst decreased after each use as shown in **Figure 6 (a)**. The activity in first usage of catalyst is accepted as 100% and decreased from 81±4 to 55±4% after 2nd, and 5th use, respectively. The explanation of decrease in the activity% of Arg-CD⁺ catalyst is deprotonation of amine groups on Arg-CD⁺ catalyst, or the accumulation, reaction by-product, $NaBO_2$ on the active sides of the catalyst reducing the catalytic performance,[34,35] the methoxy borate ($[B(OCH_3)_4]^-$) anions which is by-product of reaction can poison or deactivate the catalyst. Even with the decrease on the activity% of catalyst, Arg-CD⁺ catalysts exhibited more than 50% activity after 5 successive uses.

The regeneration ability of Arg-CD⁺ catalyst was achieved with a simple HCl acid treatment that is protonation of the amine groups on catalyst again. The regeneration studies of the Arg-CD⁺ catalyst after 5 successive uses in reaction up to 4 regeneration is given in **Figure 6 (b).** In the first 5 repeated use of Arg-CD⁺ catalyst in reaction, the activity% of catalyst decreased to 55±4% from the 100%, and after 1st regeneration of Arg-CD⁺ catalyst the activity% of catalyst increased to 99±0.9% and decreased to 69±2% after 5th use. The activity% of Arg-CD⁺ catalyst increased from 69±2% to 91±1% after 2nd regeneration, and the after 5 consecutive usages activity% of catalyst decreased to 56±3%. The activity% of catalyst increased to 89±3% after 3rd regeneration, and its 5 consecutive usages caused decrease on activity to 56±3%. The 4th regeneration after 4th reuse of Arg-CD⁺ catalyst increased activity to 65±4%, and

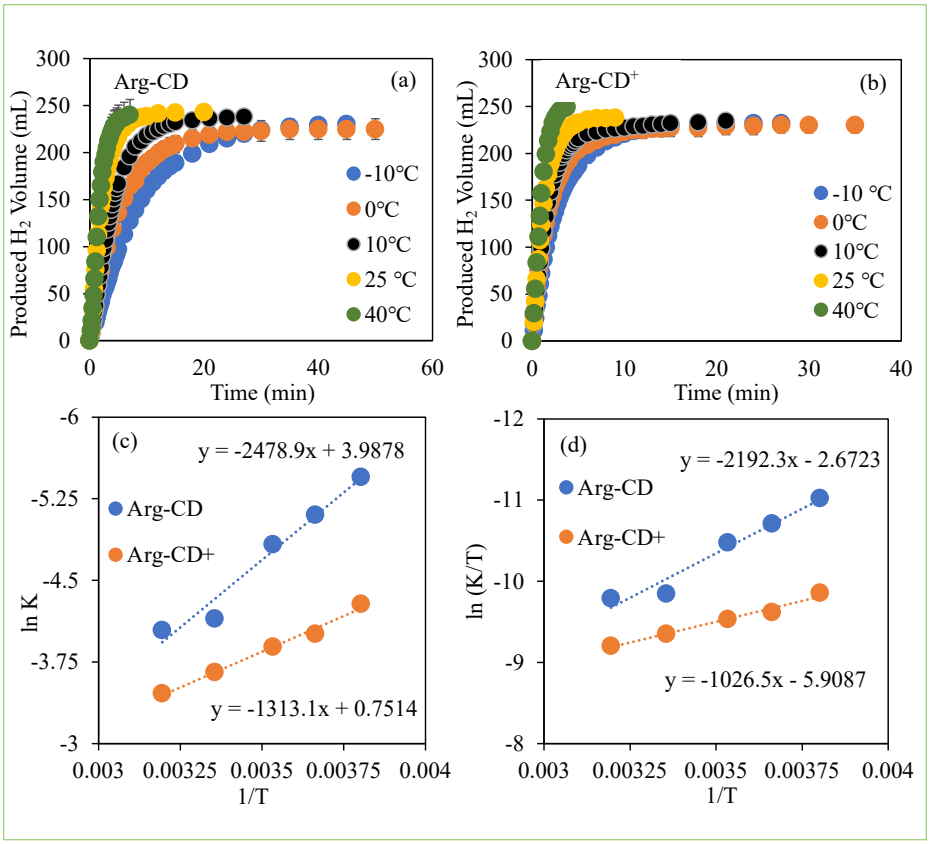

Figure 5. The effect of temperature on (a) Arg-CD, (b) Arg-CD⁺ catalyzed methanolysis of $NaBH_4$, (c) Arrhenius, and (d) Eyring plots for Arg-CD based catalysts catalyzed reactions. [Reaction condition: 20 mL methanol, 0.0965 g $NaBH_4$, 50 mg catalyst, 1000 rpm].

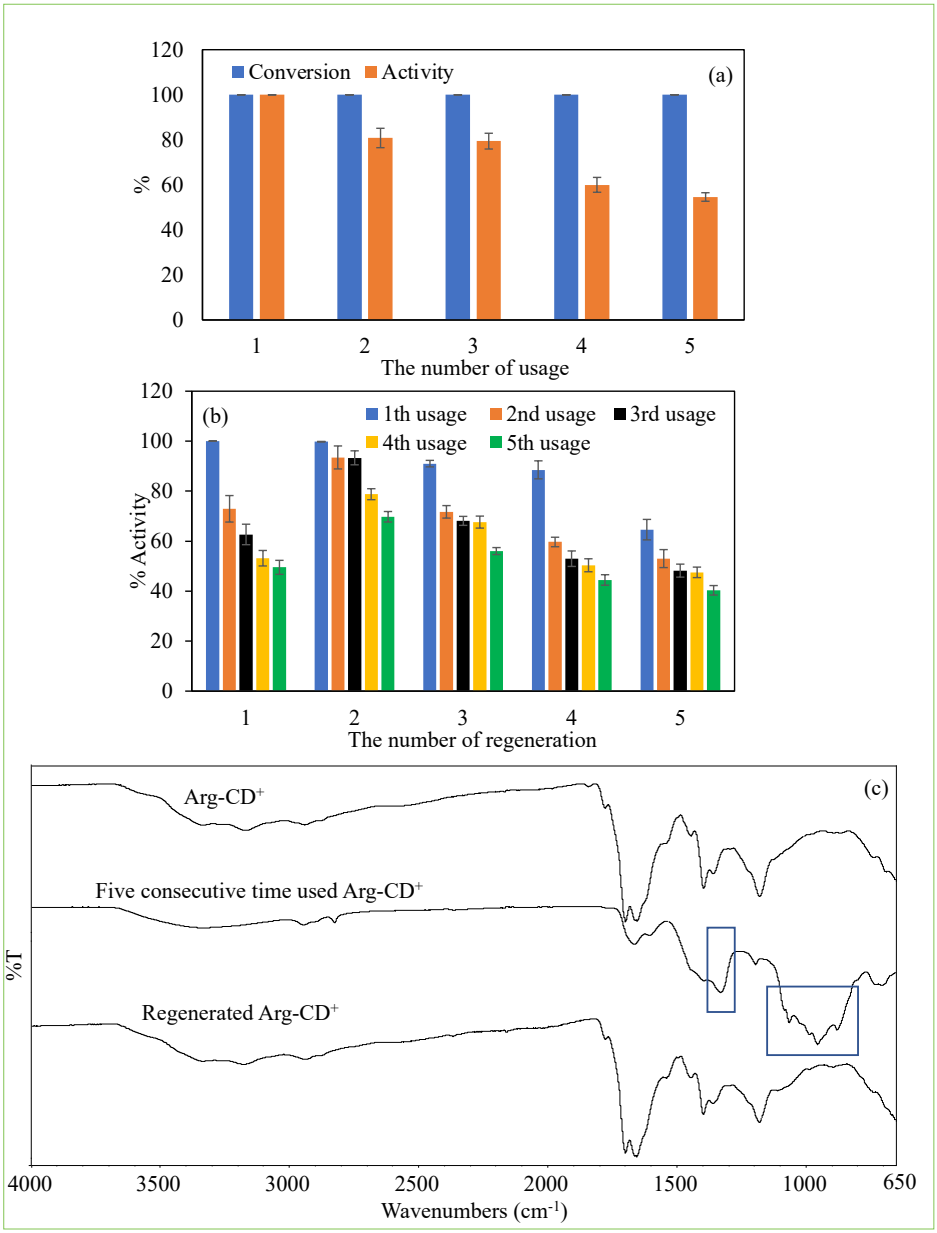

Figure 6. (a) Reuse, (b) regeneration ability of Arg-CD⁺ catalyst in methanolysis of $NaBH_4$, and (c) the FT-IR spectrum of Arg-CD⁺, 5 times used Arg-CD⁺, and regenerated Arg-CD⁺ catalyst. [Reaction condition, 20 ml methanol, 0.0965 g of $NaBH_4$, 50 mg catalyst, 1000 rpm, 25 °C].

after 5 consecutive usages activity% of catalyst decreased to 40±2%. As can be seen from **Figure 6 (b)**, a simple one step acid treatment provides easily increasing on the decreased activity% of Arg-CD⁺ after 5 consecutive uses. More than 20 usages were provided by Arg-CD⁺ catalysts in reaction to produce H_2 via enhanced regeneration ability of catalysts.

The FT-IR spectra of Arg-CD⁺ before and after five consecutive use and after regeneration are compared presented in **Figure 6 (c)** to explain possible reasons of decreasing catalytic activity after reuse and increase for the catalytic activity after acid treatment. FT-IR spectrum of five repeated used Arg-CD⁺ has the characteristic beaks for methoxy borate around 1330 cm^{-1} assigned to B-O, and the peaks between 1100-800 cm^{-1} assigned to C-O and C-H peaks. On the other hand, after the regeneration of Arg-CD⁺ catalyst the peaks belonging to methoxy borate disappeared confirming the removal of reaction byproducts. Therefore, this regeneration ability of Arg-CD⁺ catalyst makes them superior in comparison to the other catalysts used for the same purpose.

4. Conclusions

The Arg-CD prepared by microwave technique was used as catalyst in methanol to produce H_2 from $NaBH_4$. It was shown that the protonation of Arg-CDs via simple HCl treatment (Arg-CD⁺) increases the catalytic performance two-fold. Also, the calculated activation energy for Arg-CD⁺ catalyzed reaction is 10. kJ/mol is lower than most of the reported values of the different catalysts including metal and non-metal-based catalyst used for the same purpose. It was also found that the Arg-CD⁺ catalyst can be readily used in 5 consecutive runs in the reaction with more than 50% activity. The decrease in activity of Arg-CD⁺ catalyst after 5 consecutive usages is explained by the deprotonation of amine groups or the accumulation of the by-product of hydrolysis reaction, sodium metaborate ($NaBO_2$) on active sides of catalyst. On the other hand, the regeneration of the catalyst by simple acid treatment (protonation) of the used Arg-CD⁺ catalyst revealed a recovery of the catalytic activity of catalyst by reactivation of the amine groups and removing of by-product from catalyst. This simple regeneration ability of catalyst grants almost 25 repetitive usages with more than 50% activity for the reaction to produce H_2. In addition to the non-toxic nature of Arg-CD⁺ catalysts, the lower activation energy, higher reuse ability enables these Arg-CD⁺ catalysts to be a promising catalytic material for industrial applications for H_2 production from $NaBH_4$.

Conflicts of Interest: The authors declare no conflict of interest.

Acknowledgements: The authors are thankful to Erva Uslu for the support during some of the experimental studies.

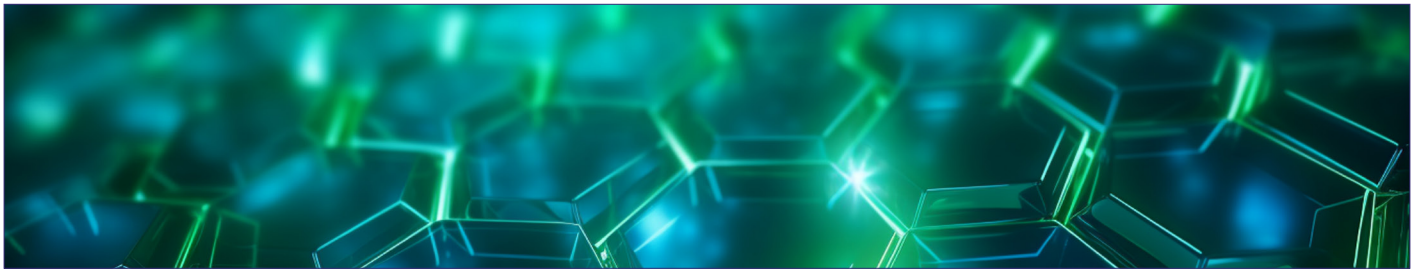

References

(1) Abdin, Z.; Zafaranloo, A.; Rafiee, A.; Mérida, W.; Lipiński, W.; Khalilpour, K. R. Hydrogen as an Energy Vector. *Renew. Sustain. Energy Rev.* **2020**, *120*, 109620. https://doi.org/10.1016/j.rser.2019.109620.

(2) Ekins, P.; Hughes, N. The Prospects for a Hydrogen Economy (1): Hydrogen Futures. *Technol. Anal. Strateg. Manag.* **2009**, *21* (7), 783–803. https://doi.org/10.1080/09537320903182264.

(3) Muir, S. S.; Yao, X. Progress in Sodium Borohydride as a Hydrogen Storage Material: Development of Hydrolysis Catalysts and Reaction Systems. *Int. J. Hydrogen Energy* **2011**, *36* (10), 5983–5997. https://doi.org/10.1016/j.ijhydene.2011.02.032.

(4) Yue, M.; Lambert, H.; Pahon, E.; Roche, R.; Jemei, S.; Hissel, D. Hydrogen Energy Systems: A Critical Review of Technologies, Applications, Trends and Challenges. *Renew. Sustain. Energy Rev.* **2021**, *146*, 111180. https://doi.org/10.1016/j.rser.2021.111180.

(5) Edwards, P. .; Kuznetsov, V. .; David, W. I. . Hydrogen Energy. *Philos. Trans. R. Soc. A Math. Phys. Eng. Sci.* **2007**, *365* (1853), 1043–1056. https://doi.org/10.1098/rsta.2006.1965.

(6) Kayfeci, M.; Keçebaş, A.; Bayat, M. Hydrogen Production. In *Solar Hydrogen Production*; Elsevier, 2019; pp 45–83. https://doi.org/10.1016/B978-0-12-814853-2.00003-5.

(7) Zhang, T.; Uratani, J.; Huang, Y.; Xu, L.; Griffiths, S.; Ding, Y. Hydrogen Liquefaction and Storage: Recent Progress and Perspectives. *Renew. Sustain. Energy Rev.* **2023**, *176*, 113204. https://doi.org/10.1016/j.rser.2023.113204.

(8) Kalenchuk, A. N.; Bogdan, V. I. Catalytic Hydrogen Storage Systems Based on Hydrogenation and Dehydrogenation Reactions. *Catal. Ind.* **2023**, *15* (2), 165–174. https://doi.org/10.1134/S2070050423020083.

(9) Chen, Y.; Kim, H. Use of a Nickel-Boride–Silica Nanocomposite Catalyst Prepared by in-Situ Reduction for Hydrogen Production from Hydrolysis of Sodium Borohydride. *Fuel Process. Technol.* **2008**, *89* (10), 966–972. https://doi.org/10.1016/j.fuproc.2008.04.005.

(10) Kirk, J.; Kim, Y.; Lee, Y.-J.; Kim, M.; Min, D.-S.; Soon Kim, P.; Hui Seo, J.; Kim, Y.; Lee, J.; Woo Choung, J.; Sohn, H.; Nam, S.-W.; Yoon, C.-W.; Kim, Y.; Jeong, H. Pushing the Limits of Sodium Borohydride Hydrolysis for On-Board Hydrogen Generation Systems. *Chem. Eng. J.* **2023**, *466*, 143233. https://doi.org/10.1016/j.cej.2023.143233.

(11) Moussa, G.; Moury, R.; Demirci, U. B.; Şener, T.; Miele, P. Boron-Based Hydrides for Chemical Hydrogen Storage. *Int. J. Energy Res.* **2013**, *37* (8), 825–842. https://doi.org/10.1002/er.3027.

(12) Hamilton, C. W.; Baker, R. T.; Staubitz, A.; Manners, I. B–N Compounds for Chemical Hydrogen Storage. *Chem. Soc. Rev.* **2009**, *38* (1), 279–293. https://doi.org/10.1039/b800312m.

(13) Akkus, M. S. The Catalytic Performance of Nanorod Nickel Catalyst in the Hydrolysis of Lithium Borohydride and Dimethylamine Borane. *Catalysts* **2023**, *13* (3), 458. https://doi.org/10.3390/catal13030458.

(14) Zhang, E.; Xu, R.; Wang, L.; Chen, J.; Zhang, B.; Wang, G. One-Pot Synthesis of Magnetic Copper Ferrite Nanocubes for Hydrogen Production by Hydrolysis of Sodium Borohydride. *Ceram. Int.* **2023**, *49* (14), 23464–23470. https://doi.org/10.1016/j.ceramint.2023.04.178.

(15) Yang, N.; Yao, H.; Bu, F.; Gu, M.; Zhao, X.; Huang, L.; Zhao, C.; Cheng, Y.; Zhang, J. Hydrolysis Kinetics of LiAlH 4 at Subzero Temperatures. *ACS Appl. Energy Mater.* **2023**, *6* (4), 2550–2558. https://doi.org/10.1021/acsaem.2c04007.

(16) Kobayashi, Y.; Sunada, Y. Germanium Hydrides as an Efficient Hydrogen-Storage Material Operated by an Iron Catalyst. *Chem. Sci.* **2023**, *14* (5), 1065–1071. https://doi.org/10.1039/D2SC06011F.

(17) Dragan, M. Hydrogen Storage in Complex Metal Hydrides NaBH4: Hydrolysis Reaction and Experimental Strategies. *Catalysts* **2022**, *12* (4), 356. https://doi.org/10.3390/catal12040356.

(18) Han, M.; Qu, J.; Guo, Q. Corn Stalk Activated Carbon Based Co Catalyst Prepared by One-Step Method for Hydrogen Generation. *Procedia Eng.* **2015**, *102*, 450–457. https://doi.org/10.1016/j.proeng.2015.01.186.

(19) Cao, S.; Yu, J. Carbon-Based H2-Production Photocatalytic Materials. *J. Photochem. Photobiol. C Photochem. Rev.* **2016**, *27*, 72–99. https://doi.org/10.1016/j.jphotochemrev.2016.04.002.

(20) Brack, P.; Dann, S. E.; Wijayantha, K. G. U. Heterogeneous and Homogenous Catalysts for Hydrogen Generation by Hydrolysis of Aqueous Sodium Borohydride (NaBH 4) Solutions. *Energy Sci. Eng.* **2015**, *3* (3), 174–188. https://doi.org/10.1002/ese3.67.

(21) Konwar, L. J.; Boro, J.; Deka, D. Review on Latest Developments in Biodiesel Production Using Carbon-Based Catalysts. *Renew. Sustain. Energy Rev.* **2014**, *29*, 546–564. https://doi.org/10.1016/j.rser.2013.09.003.

(22) Liu, X.; Chi, J.; Mao, H.; Wang, L. Principles of Designing Electrocatalyst to Boost Reactivity for Seawater Splitting. *Adv. Energy Mater.* **2023**. https://doi.org/10.1002/aenm.202301438.

(23) Ham, Y.; Kim, C.; Shin, D.; Kim, I.; Kang, K.; Jung, Y.; Lee, D.; Jeon, S. All-Graphene Quantum Dot-Derived Battery: Regulating Redox Activity Through Localized Subdomains. *Small* **2023**. https://doi.org/10.1002/smll.202303432.

(24) Xia, C.; Zhu, S.; Feng, T.; Yang, M.; Yang, B. Evolution and Synthesis of Carbon Dots: From Carbon Dots to Carbonized Polymer Dots. *Adv. Sci.* **2019**, *6* (23), 1901316. https://doi.org/10.1002/advs.201901316.

(25) Kang, Z.; Lee, S.-T. Carbon Dots: Advances in Nanocarbon Applications. *Nanoscale* **2019**, *11* (41), 19214–19224. https://doi.org/10.1039/C9NR05647E.

(26) Cui, H.; Ye, Y.; Liu, T.; Alothman, Z. A.; Alduhaish, O.; Lin, R.-B.; Chen, B. Isoreticular Microporous Metal–Organic Frameworks for Carbon Dioxide Capture. *Inorg. Chem.* **2020**, *59* (23), 17143–17148. https://doi.org/10.1021/acs.inorgchem.0c02427.

(27) To, D. T. H.; Park, J. Y.; Yang, B.; Myung, N. V.; Choa, Y.-H. Nanocrystalline ZnO Quantum Dot-Based Chemiresistive Gas Sensors: Improving Sensing Performance towards NO2 and H2S by Optimizing Operating Temperature. *Sensors and Actuators Reports* **2023**, *6*, 100166. https://doi.org/10.1016/j.snr.2023.100166.

(28) Qi, Y.; Zhao, J.; Wang, H.; Zhang, A.; Li, J.; Yan, M.; Guo, T. Shaddock Peel-Derived N-Doped Carbon Quantum Dots Coupled with Ultrathin BiOBr Square Nanosheets with Boosted Visible Light Response for High-Efficiency Photodegradation of RhB. *Environ. Pollut.* **2023**, *325*, 121424. https://doi.org/10.1016/j.envpol.2023.121424.

(29) Suner, S. S.; Sahiner, M.; Yilmaz, A. S.; Ayyala, R. S.; Sahiner, N. Light-Activated Modified Arginine Carbon Dots as Antibacterial Particles. *Catalysts* **2022**, *12* (11), 1376. https://doi.org/10.3390/catal12111376.

(30) Suner, S. S.; Sahiner, M.; Ayyala, R. S.; Bhethanabotla, V. R.; Sahiner, N. Nitrogen-Doped Arginine Carbon Dots and Its Metal Nanoparticle Composites as Antibacterial Agent. *C—Journal Carbon Res.* **2020**, *6* (3), 58. https://doi.org/10.3390/c6030058.

(31) Demirci, S.; Sunol, A. K.; Sahiner, N. Catalytic Activity of Amine Functionalized Titanium Dioxide Nanoparticles in Methanolysis of Sodium Borohydride for Hydrogen Generation. *Appl. Catal. B Environ.* **2020**, *261*, 118242. https://doi.org/10.1016/j.apcatb.2019.118242.

(32) Petrosyan, A. M. Vibrational Spectra of L-Arginine Tetrafluoroborate and l-Arginine Perchlorate. *Vib. Spectrosc.* **2006**, *41* (1), 97–100. https://doi.org/10.1016/j.vibspec.2006.01.009.

(33) Sunatkari, S. Study of Structural and Spectroscopic Characterization of Co-Doped ZnS Nanoparticles Capped with L-Arginine. *J. Phys. Conf. Ser.* **2023**, *2426* (1), 012036. https://doi.org/10.1088/1742-6596/2426/1/012036.

(34) Hagen, J. *Concepts of Modern Catalysis and Kinetics Catalysis from A to Z Principles and Practice of Heterogeneous Catalysis Catalytic Membranes and Membrane Reactors Spectroscopy in Catalysis*; 2006.

(35) GARRON, A.; SWIERCZYNSKI, D.; BENNICI, S.; AUROUX, A. New Insights into the Mechanism of H2 Generation through NaBH4 Hydrolysis on Co-Based Nanocatalysts Studied by Differential Reaction Calorimetry. *Int. J. Hydrogen Energy* **2009**, *34* (3), 1185–1199. https://doi.org/10.1016/j.ijhydene.2008.11.027.

(36) Saka, C. Sulphur and Nitrogen-Doped Metal-Free Microalgal Carbon Catalysts for Very Active Dehydrogenation of Sodium Borohydride in Methanol. *Int. J. Hydrogen Energy* **2021**, *46* (35), 18326–18337. https://doi.org/10.1016/j.ijhydene.2021.03.001.

(37) Kaya, S.; Saka, C.; Yildiz, D.; Erol, S.; Ulas, B.; Demir, I.; Kivrak, H. Enhanced Hydrogen Production via Methanolysis and Energy Storage on Novel Poplar Sawdust-Based Biomass-Derived Activated Carbon Catalyst. *J. Appl. Electrochem.* **2023**, No. 0123456789. https://doi.org/10.1007/s10800-023-01873-4.

(38) Saka, C. Facile Fabrication of P-Doped g-C3N4 Particles with Nitrogen Vacancies for Efficient Dehydrogenation of Sodium Borohydride Methanolysis. *Fuel* **2022**, *313* (November 2021), 122688. https://doi.org/10.1016/j.fuel.2021.122688.

(39) Samatya Ölmez, S.; Balbay, A.; Saka, C. Phosphorus Doped Carbon Nanodots Particles Based on Pomegranate Peels for Highly Active Dehydrogenation of Sodium Borohydride in Methanol. *Int. J. Hydrogen Energy* **2022**, *47* (74), 31647–31655. https://doi.org/10.1016/j.ijhydene.2022.07.091.

(40) Wang, F.; Zhang, Y.; Luo, Y.; Wang, Y.; Zhu, H. Preparation of Dandelion-like Co–Mo–P/CNTs-Ni Foam Catalyst and Its Performance in Hydrogen Production by Alcoholysis of Sodium Borohydride. *Int. J. Hydrogen Energy* **2020**, *45* (55), 30443–30454. https://doi.org/10.1016/j.ijhydene.2020.08.037.

(41) Wang, F.; Zhang, Y.; Wang, Y.; Luo, Y.; Chen, Y.; Zhu, H. Co-P Nanoparticles Supported on Dandelion-like CNTs-Ni Foam Composite Carrier as a Novel Catalyst for Hydrogen Generation from NaBH4 Methanolysis. *Int. J. Hydrogen Energy* **2018**, *43* (18), 8805–8814. https://doi.org/10.1016/j.ijhydene.2018.03.140.

(42) Eken Korkut, S.; Küçükkeçeci, H.; Metin, Ö. Mesoporous Graphitic Carbon Nitride/Black Phosphorus/AgPd Alloy Nanoparticles Ternary Nanocomposite: A Highly Efficient Catalyst for the Methanolysis of Ammonia Borane. *ACS Appl. Mater. Interfaces* **2020**, *12* (7), 8130–8139. https://doi.org/10.1021/acsami.9b18917.